**Jurnal Fitofarmaka Indonesia**, 2021; 8(3) 5-11
http://jurnal.farmasi.umi.ac.id/index.php/fitofarmakaindo/index

# Radiolabeled Curcumin as *β* Amyloid Imaging and Tumor Targeting Imaging Agents

**Nurmaya Effendi**
Institute for Frontier Science Initiative, Kanazawa University, Kakuma-machi, Kanazawa, Ishikawa
Faculty of Pharmacy, Universitas Muslim Indonesia, Indonesia

**Article info**
**History**
*Submission*: 28-10-2020
*Review*: 20-12-2020
*Accepted*: 24-02-2021

***Email:**
nurmaya82@gmail.com

**DOI:** 10.33096/jffi.v7i3.708

**Keywords:**
*Curcumin; radiolabeled; β amyloid imaging; tumor-imaging agent*

**Abstract**
*Curcumin, a polyphenolic compound, derived from the rhizomes of Curcuma longa L. Curcumin shows potential pharmacological action against numerous disorders, including cancer, neurodegenerative, and infection diseases. Curcumin-based molecular imaging agents could be useful for early detection of Alzheimer's Disease and tumor and monitor the progress of therapy. Radiolabeled curcumin and its derivatives become promising compounds as imaging agents. In this review, radiolabeled curcumin bearing radionuclides including Fluorine-18, Technetium-99m, Iodine-125, and Gallium-68 are reviewed as an effort to develop curcumin-based probes not only for β amyloid imaging but also for tumor imaging.*

## I. Introduction

The accumulation of β-amyloid (Aβ) aggregates and neurofibrillary tangles in human brain are still considered some of the key features for neurodegenerative disorder namely Alzheimer's disease (AD) (Uzuegbunam, Librizzi and Yousefi, 2020). Histological examination of brain sample is still required to assign a definitive diagnosis of AD (Takizawa *et al.*, 2015). However, using cerebrospinal fluid (CSF) biomarkers and positron emission tomography (PET) agents of patient which combined with several new clinical criteria, AD can be early diagnosed and monitored (Budson and Solomon, 2012; Jack *et al.*, 2018). PET imaging is a non-invasive imaging technique that allows identifying the patients who are at risk of developing AD, and also to monitor disease progression or both (Steven T DeKosky and Marek, 2003; Reiman and Jagust, 2012). Hence, PET imaging agent may serve as an attractive diagnostic tool to monitor disease progression and the interaction of ligands with their targets (Bailey *et al.*, 2005). Aβ is the most studied and first target for the neuroimaging of AD (Filippi *et al.*, 2018), hence it is no surprise that there are already selective PET radiotracers for its imaging. Food and Drug Administration (FDA) approved Amyvid ([$^{18}$F]florbetapir), Neuraceq ([$^{18}$F]florbetaben), and Vizamyl ([$^{18}$F]flutemetamol) (Figure 1) as PET radiotracer for AD.

Recently, several studies reported that curcumin showed high affinity toward Aβ plaques. Curcumin, 1,7-bis(4-hydroxy-3-methoxyphenyl)-1,6-heptadiene-3,5-dione, is a yellow-polyphenol pigment isolated from the rhizomes of *Curcuma longa* L and commonly known as turmeric (Hewlings and Kalman, 2017). The structure of curcumin shown in Figure 1. Curcumin has a wide spectrum of pharmacological actions and it has been reported to have anti-inflammatory (Zhu *et al.*, 2014), anti-microbial (Chen *et al.*, 2016), anti-oxidant (Banez *et al.*, 2020), anti-carcinogenic (Perrone *et al.*, 2015; Zhao *et al.*, 2017; Walker and Mittal, 2020) activities. Because of its distinctive uptake in normal and cancer cells (Kunwar *et al.*, 2008; Heger *et al.*, 2014), radiolabeled curcumin is one of attractive agents for tumor targeting radiopharmaceuticals. The present work introduces radiolabeled curcumin and its derivatives focusing on radiotracers for cancer and Aβ imaging.

## II. Research Method

### II.1 Radiolabeled curcumin

Molecular imaging is a type of non-invasively medical imaging that allows to visualize, characterize, and measure the biological processes at molecular and cellular levels (Mankoff, 2007). Nuclear medicine is a revolutionized invention in diagnostic imaging using radiopharmaceuticals because it can be utilized to diagnose diseases noninvasively and facilitate monitoring disease progression or response to treatment of therapy repeatedly. Using single photon-emission computed tomography (SPECT) and PET imaging the diagnosis and progress of therapy the molecular target can be assessed (Fass, 2008; Cunha *et al.*, 2014). SPECT has some merits such as low cost and more assessable than PET, even though PET has better sensitivity and resolution (Galbán *et al.*, 2010). Due to its pharmacological and biological

actions, radiolabeled curcumin and their derivatives could be potential biomarkers for imaging of Alzheimer's disease and cancer by means of nuclear medicine imaging techniques which could be useful for early detection of them and contribute to personalized medicine.

As promising compound, radiolabeled curcumin and its derivatives have been developed and evaluated their feasibilities as imaging agents. Radiogallium (Orteca *et al.*, 2019) and radioiodinated (Kumar, Subramanian and Samuel, 2016) curcumin have been reported as cancer imaging agents. Other studies showed the $^{99m}$Tc (Sagnou *et al.*, 2011) and $^{18}$F (Kim *et al.*, 2019) labeled curcumin have been used as β-amyloid plaques imaging agents.

## III. Results and Discussion

### III.1 $^{18}$F-curcumin

Fluorine-18 ($^{18}$F) is one of PET radionuclides that routinely utilized in radiolabeling of biomolecules with half-life of 109.8 min (Alauddin, 2012). High spatial resolution and high sensitivity are two vaporable properties of PET imaging agent. However, high cost in preparation limited its use. Radiofluorinated-curcumin as imaging agents have been developed as detailed follow:

1. ***1-[4-(3-[$^{18}$F]Fluoropropoxy)-3-methoxyphenyl]-5-hydroxy-7-(4-hydroxy-3-methoxyphenyl)-1,4,6-heptatrien-3-one ([$^{18}$F]FPC)***

Ryu et al. synthesized eight curcumin and its derivatives and evaluated their binding affinity for Aβ plaques. The binding affinity ($K_i$) of FPC to Aβ aggregates was 0.07 nM. The accumulation of [$^{18}$F]FPC (Figure 2) in the mice brine 2 min and 30 min after injection was 0.5 %ID/g and 0.11 %ID/gram respectively. This probe was metabolically stable in brain. Therefore, [$^{18}$F]FPC exhibited potential probes as Aβ imaging agent (Ryu *et al.*, 2006). However, [$^{18}$F]FPC has poor brain permeability may be caused by its fast metabolism in liver and intestine.

2. ***[$^{18}$F]1-(4-[$^{18}$F]Fluoroethyl)-7-(4'-methyl)curcumin ([$^{18}$F]FEC)***

Lee and group synthesized five curcumin derivatives and their binding affinities for Aβ (1-40) aggregates have been evaluated. The binding affinity ($K_i$) of FEC was 2.12 nM. Subsequently, accumulation of radiofluorinated 1-(4-fluoroethyl)-7-(4′-methyl)curcumin (Figure 2) in normal mice brain was 1.44 and 0.45 %ID/gram at 2 and 30 min post-injection, respectively. This result indicated that [$^{18}$F]FEC has better brain permeability than ([$^{18}$F]FPC) (Lee *et al.*, 2011).

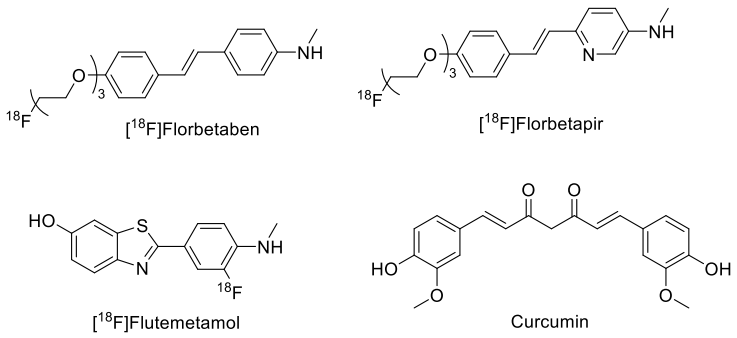


**Figure 1**. The chemical structure of [$^{18}$F]florbetapir, [$^{18}$F]florbetaben, [$^{18}$F]flutemetamol, and curcumin

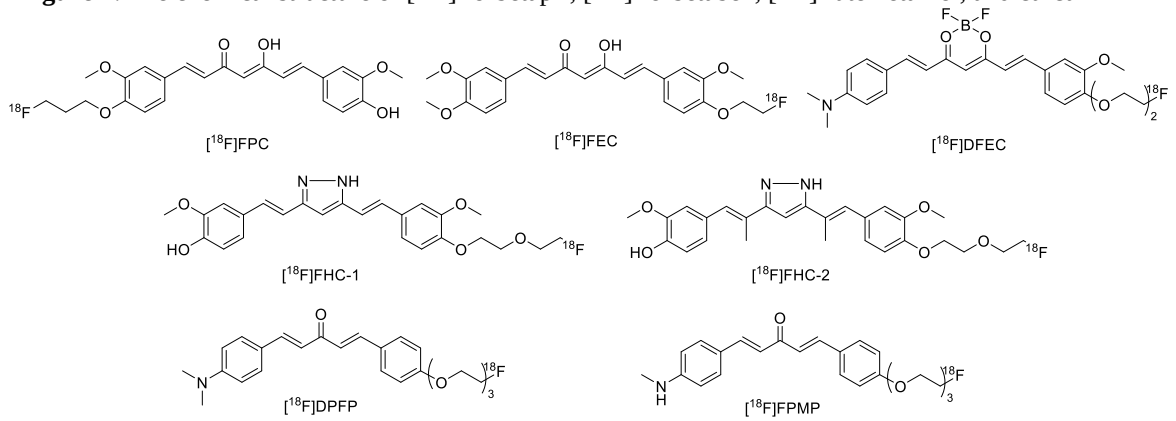


**Figure 2.** The chemical structure of [$^{18}$F]FPC, [$^{18}$F]FEC, [$^{18}$F]DFEC, [$^{18}$F]FHC-1, [$^{18}$F]FHC-2, [$^{18}$F]DPFP, and [$^{18}$F]FPMP

***3. [$^{18}$F]4′-dimethylamino-4″-(2-(2-fluoroethoxy)ethoxy) curcuminoid ([$^{18}$F]DFEC)***

In 2019, Kim at al. reported four difluoroboron-curcumin derivatives and selected one of them to be evaluated its feasibility as Aβ imaging agent, namely 4′-dimethylamino-4″-(2-(2-fluoroethoxy)ethoxy) curcuminoid. In that study, [$^{18}$F]DFEC as seen in Figure 2 was selected for further *in vitro* and *in vivo* evaluations based on binding affinity ($K_d$) value for Aβ(1-40) aggregates (19.66 nM) and feasibility for radiofluorinated labeling. [$^{18}$F]DFEC exhibited high *in vitro* stability. In addition, low accumulation of [$^{18}$F]DFEC in femur indicated that this probe was *in vivo* stable. Low initial brain uptake in biodistribution result at 2 min post-injection (0.49 %ID/gram) and delay wash-out from the brine (1.19 %ID/gram at 60 min post-injection) has been reported (Kim *et al.*, 2019).

***4. [$^{18}$F]F-labeled dibenzylideneacetone derivatives ([$^{18}$F]FHC)***

Using structure activity relationship (SAR) Cui et al. synthesized and evaluated two radiofluorinated curcumin derivatives which have high affinity for Aβ aggregates. There are (1*E*,4*E*)-1-(4-(dimethylamino)phenyl)-5-(4-(2-(2-(2-fluoroethoxy)-ethoxy)ethoxy)phenyl)penta-1,4-dien-3-one (DPFP) and (1*E*,4*E*)-1-(4-(2-(2-(2-fluoroethoxy)ethoxy)ethoxy)phenyl)-5-(4-(methylamino)phenyl)penta-1,4-dien-3-one (FPMP) with $K_i$ value were 6.9 ± 1.4 nM and 8.6 ± 1.3 nM, respectively. Radiofluorinated compounds, [$^{18}$F]DPFP and [$^{18}$F]FPMP (Figure 2), have log *D* value were 2.97 and 3.08, respectively. Both radiofluorinated compounds has initial brain uptake at 2 min post-injection about 4.13 ± 0.41 and 5.15 ± 0.17 %ID/gram. At 30 min post-administration the probes retained about 1.04 and 1.35 %ID/gram in mice brine (Cui *et al.*, 2011).

***5. [$^{18}$F]F-labeled hydrazinocurcumin derivative ([$^{18}$F]FHC)***

In 2015, Shin at al. reported their studies in preparation of radiofluorinated hydrazinocurcumin derivatives (Figure 3). This probe was accumulated in human umbilical vascular endothelial cells and rat C6 glioma cells. Biodistribution data exhibited that [$^{18}$F]FHC-2 accumulated in tumor of C6 glioma-xenograft mice (3.20 ± 0.35% ID/gram vs 0.98 ± 0.31% ID per g for [$^{18}$F]FHC-1) at 30 min post-injection. The accumulation of [$^{18}$F]FHC-2 in C6 glioma-tumor model mice could be visualized clearly using PET camera, which cannot be shown by [$^{18}$F]FHC-1.can be seen in Table 2 and Figure 2.

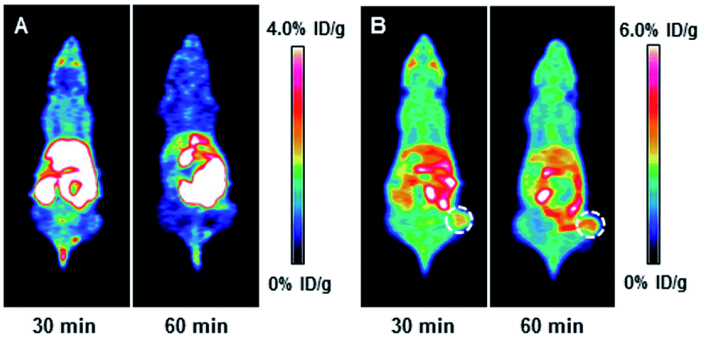


**Figure 3**. Dynamic small animal PET images of (A) [$^{18}$F]FHC-1 and (B) [$^{18}$F]FHC-2 in glioma tumor-bearing mice modified from Shin et al. (Shin *et al.*, 2015), reproduced by permission of The Royal Society of Chemistry

**III.2 $^{99m}$Tc-curcumin**

Technetium-99m ($^{99m}$Tc) is generated by transportable $^{99}$Mo-$^{99m}$Tc generator, readily available, and inexpensive. $^{99m}$Tc is an attractive radionuclide for SPECT imaging due to its favorable physical and chemical properties, such as a low *γ*-rays emission (140 keV, 89% abundance) and a moderate half-life (6 h) which is sufficient for preparation of $^{99m}$Tc-based radiopharmaceuticals (International Atomic Energy Agency (IAEA), 2009; Boschi, Uccelli and Martini, 2019). $^{99m}$Tc-labeled curcumin as Aβ imaging agents have been reported, some of them detailed as below:

***1. fac-[$^{99m}$Tc(CO)$_3$(curcu)-(imi)] and fac-[$^{99m}$Tc(CO)$_3$(curcu)-(isc)]***

Sagnou et al. reported two novels $^{99m}$Tc-labeled curcumin derivatives, *fac*-$^{99m}$Tc(CO)$_3$(curcu)-(imi) and *fac*-$^{99m}$Tc(CO)$_3$(curcu)-(isc) (Figure 4) using ″2+1″ ligand system. This group synthesized and characterized ″2+1″ complexes of the [M(CO)$_3$] (M = Re and $^{99m}$Tc) core with curcumin as bidentate OO ligands and imidazole (imi) and isocyanocyclohexane (isc) as monodentate ligands. *In vitro* binding affinity of non-radioactive rhenium labeled curcumin complexes was performed using Alzheimer′s disease brain slices to assess their feasibilities as Aβ imaging agents. The fluorescence microscope image visualized clearly the plaques of human AD brine slices, despite the significant difference in their fluorescence intensity was found (Sagnou *et al.*, 2011).

***2. fac-[$^{99m}$Tc/Re(cur)-(PPh$_3$)$_2$(CO)$_2$] and fac-[$^{99m}$Tc/Re(cur)-(PPh$_3$)(CO)$_3$]***

In 2013, Triantis et al. reported the preparation the non-radiolabeled (Rhenium

complexes) and radiolabeled ($^{99m}$Tc complexes) of curcumin derivatives, *fac*-[$^{99m}$Tc/Re(cur)-$(PPh_3)_2(CO)_2$] and *fac*-[$^{99m}$Tc/Re(cur)-$(PPh_3)(CO)_3$] (Figure 4). Using ″2+1″ ligand system, they synthesized both curcumin-based probes, wherein phosphine utilized as the monodentate ligand and complexes of the *fac*-$[M(CO)_3]$ (M = Re and $^{99m}$Tc) core with curcumin as bidentate OO ligand. *In vitro* staining of human post-mortem AD brain sections with rhenium-curcumin complexes which visualized under the fluorescence microscope exhibited both complexes bind selectivity to the plaques (Triantis *et al.*, 2013).

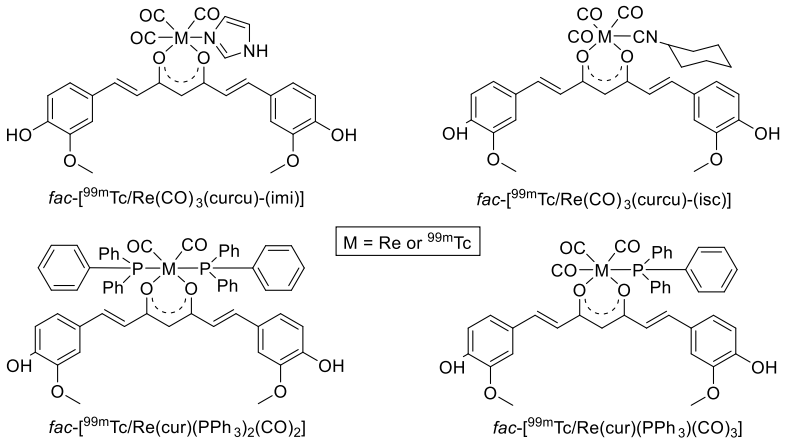


**Figure 4.** The chemical structure of *fac*-[$^{99m}$Tc/Re$(CO)_3$(curcu)-(imi)], *fac*-[$^{99m}$Tc/Re$(CO)_3$(curcu)-(isc)], *fac*-[$^{99m}$Tc/Re(cur)-$(PPh_3)_2(CO)_2$], and *fac*-[$^{99m}$Tc/Re(cur)-( $PPh_3)(CO)_3$]

### III.3 $^{125}$I-curcumin

Radionuclides of iodine have been widely used in various fields of medicinal and biological sciences. These radionuclides insert into bioactive molecules to visualize the molecular target non-invasively and to diagnose the particular disease (Effendi *et al.*, 2019). There are some types of iodine radionuclides with different type of ray emission, such as iodine-123 (SPECT), iodine-124 (PET), iodine-125 (preclinical research and Auger therapy), iodine-131 (*β*-therapy) (Dubost *et al.*, 2020). Identical chemical properties of iodine radionuclides allow the *in vitro* and *in vivo* information from one radioiodine nuclide bearing bioactive compound serve as basic data for further work (Effendi *et al.*, 2018). Radioiodine-labeled curcumin probes have been reported, some of them described as follow:

#### *1. $^{125}$I-curcumin*

In 2013, Kumar et al. reported their studies in preparation of radioiodinated curcumin as tumor-targeting probes. Using iodogen method, Iodine-125 was inserted into curcumin to obtain $^{125}$I-curcumin (Figure 5) with radiochemical yield more than 75% and high purity (>95). Accumulation of $^{125}$I-curcumin in EL4 murine lymphoma cells reached 6.8% dose/500,000 cells. The tumor uptake of $^{125}$I-curcumin in lymphoma-tumor model mice reached 3.3% ID/gram at 3 h post-injection. The biodistribution data exhibited that $^{125}$I-curcumin was washed-out slowly from blood and other non-targeted tissues (Kumar, Subramanian and Samuel, 2016).

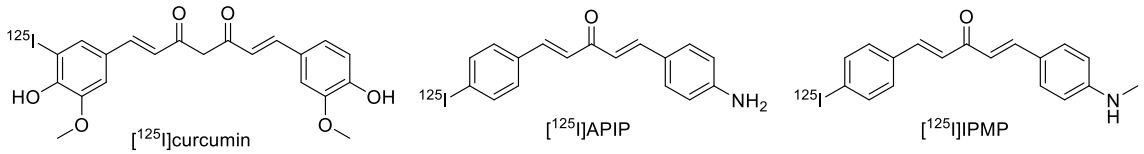


**Figure 5.** The chemical structure of [$^{125}$I]curcumin, [$^{125}$I]APIP, and [$^{125}$I]IPMP

#### *2. Radioiodinated dibenzylideneacetone derivatives*

Cui et al. synthesized two radioiodinated dibenzylideneacetone derivatives for SPECT Aβ imaging, radioiodinated (1*E*,4*E*)-1-(4-aminophenyl)-5-(4-iodophenyl)penta-1,4-dien-3-one ([$^{125}$I]APIP) and (1*E*,4*E*)-1-(4-iodophenyl)-5-(4-(methylamino)phenyl)penta-1,4-dien-3-one ([$^{125}$I]IPMP) (Figure 5) (Cui *et al.*, 2011). *In vitro* binding affinity ($K_i$) value of APIP and IPMP were 7.0 ± 2.2 nM and 2.8 ± 0.5 nM, respectively. Meanwhile, Log *D* values of [$^{125}$I]APIP and [$^{125}$I]IPMP are 3.26 ± 0.05 and 3.55 ± 0.02, respectively. Accumulation of [$^{125}$I]APIP in mice

brine at 2 post-injection were 4.56 ± 0.42 and decreased to 1.36 ± 0.19 %ID/gram at 30 min post-injection. While brain uptake of [$^{125}$I]IPMP after 2 min reached 4.68 ± 0.25 %ID/gram and after 30 min reduced to 1.38 ± 0.23 %ID/gram (Cui *et al.*, 2011).

### III.4 $^{68}$Ga-curcumin

The radionuclide $^{68}$Ga has a great potential property for clinical PET and could be an attractive alternative to $^{18}$F which require an on-site cyclotron in production. $^{68}$Ga is a generator-produced radionuclide with a half-life of 68 min. In principle, the long half-life of the parent nuclide $^{67}$Ge (270.8 days) provides a generator with a long life span (Martiniova *et al.*, 2016). Radionuclide Ga-67 usually was used in initial evaluation of radiogallium complexes due to it is an easy-to-handle radioisotope with a longer half-life (3.3 days) than $^{68}$Ga. The following is detailed some curcumin-based radiogallium probes as tumor-targeting and Aβ imaging agents.

1. ***[$^{68}$Ga] labeled curcumin and curcuminoid complexes ([$^{68}$Ga](CUR)$_2^+$, [$^{68}$Ga](bDHC)$_2^+$, and [$^{68}$Ga](DAC)$_2^+$)***

Asti and groups synthesized and characterized curcumin and curcuminoid-based radiogallium complexes, their chemical structures were displayed in Figure 6. Subsequently, they evaluated their binding affinity for Aβ and uptake in A549 lung cancer cells. [$^{68}$Ga](CUR)$_2^+$, [$^{68}$Ga](bDHC)$_2^+$, and [$^{68}$Ga](DAC)$_2^+$ were synthesized in high radiochemical yield and purity and *in vitro* stable in saline and human serum. All of probes were accumulated in A549 lung cancer cells. Meanwhile, [$^{68}$Ga](CUR)$_2^+$and [$^{68}$Ga](DAC)$_2^+$ showed high binding affinity for synthetic Aβ fibrils (Asti *et al.*, 2014).

In another year, this group (Rubagotti *et al.*, 2016) continued the evaluation of these radiogallium probes and explored their feasibility as Aβ imaging agents. They reported that [$^{68}$Ga](CUR)$_2^+$ and [$^{68}$Ga](DAC)$_2^+$ complexes have high binding affinity for synthesized Aβ fibrils and medium affinity has been shown by [$^{68}$Ga](bDHC)$_2^+$ (*in vitro* study). On the other hand, in *in vivo* study using post-mortem brain cryosections of male Tg2576 mice, all of gallium complexes could not visualize amyloid plaques. Low *in vivo* stability of complexes and a hampered passage across the blood-brain barrier might be involved in this result (Rubagotti *et al.*, 2016).

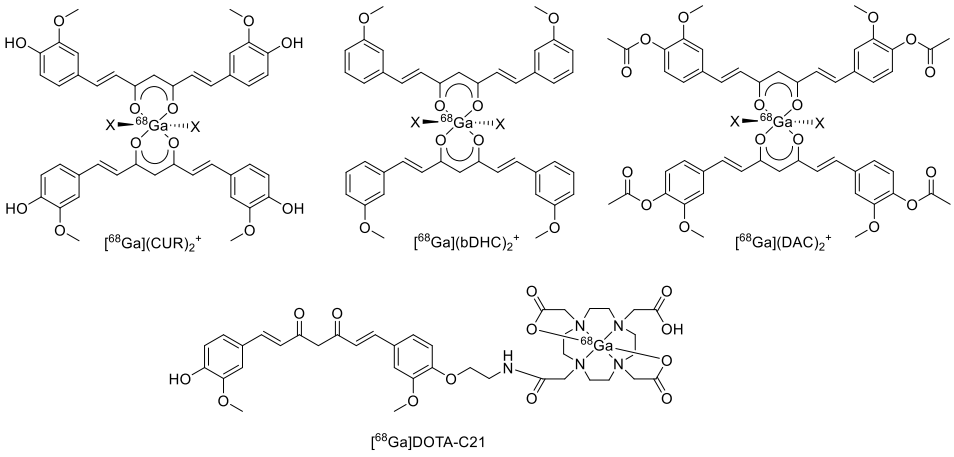


**Figure 6**. The chemical structure of [$^{68}$Ga](CUR)$_2^+$, [$^{68}$Ga](bDHC)$_2^+$, [$^{68}$Ga](DAC)$_2^+$, and [$^{68}$Ga]DOTA-C21

2. ***[$^{68}$Ga]DOTA labeled curcumin ([$^{68}$Ga]DOTA-C21)***

Orteca et al. explored curcuminoid-based radiogallium complexes as colon-rectal carcinoma imaging. [$^{68}$Ga]DOTA-C21 uptake in HT29 colorectal cancer and K562 lymphoma cells was comparable to normal human lymphocytes. Biodistribution result exhibited that [$^{68}$Ga]DOTA-C21 was accumulated in HT29 tumor-xenograft mice at 1 h post-administration (2.27 ± 0.85 %ID/gram increased to 3.57 ± 0.3 %ID/gram at 1.5 h post-injection. [$^{68}$Ga]DOTA-C21 retained for long enough in blood and some others non-targeted tissues such as small intestine, kidney, and lung (Orteca *et al.*, 2019).

## IV. Conclusions

In this review, we introduced a variety of radiolabeled curcumin as Aβ imaging or tumor-targeting imaging agents. Curcumin has a wide spectrum of biological and pharmacological actions. Anti-inflammatory, anti-microbial, anti-oxidant, and anti-carcinogenic activities of curcumin have been studied. A sufficient binding affinity of curcumin for β amyloid as one of biomarker for Alzheimer's Disease encourage curcumin become a promising compound for Aβ imaging and tumor targeting imaging. Nuclear medicine imaging as

non-invasively technique to visualize the molecular target in order to get early detection of disease and monitor the progress of treatment has attractive attention oncologist and researchers. Some promising curcumin-bearing radionuclide derivatives have been developed in recent years as introduced some of them in this review. However, structure modification of them is still needed to guarantee an appropriate imaging agent not only for Aβ imaging but also for tumor imaging. Hopefully, novel curcumin-based imaging agents with promising properties could be developed in the near future.

## V. Conflict of Interest

The author declares that there is no conflict of interest regarding the publication of this paper.

## References


Alauddin, M. M. (2012) 'Positron Emission Tomography (PET) Imaging with $^{18}$F-Based Radiotracers', *American Journal of Nuclear Medicine and Molecular Imaging*, 2(1), pp. 55–76.

Asti, M. *et al.* (2014) 'Synthesis and Characterization of $^{68}$Ga-Labeled Curcumin and Curcuminoid Complexes as Potential Radiotracers for Imaging of Cancer and Alzheimer's Disease', *Inorganic Chemistry*, 53(10), pp. 4922–4933. doi: 10.1021/ic403113z.

Bailey, D. L. *et al.* (2005) *Positron Emission Tomography. Basic Sciences*. London: UK: Springer-Verlag London Limited.

Banez, M. J. *et al.* (2020) 'A Systemic Review on The Antioxidant and Anti-inflammatory Effects of Resveratrol, Curcumin, and Dietary Nitric Oxide Supplementation on Human Cardiovascular Health', *Nutrition Research*, 78, pp. 11–26. doi: 10.1016/j.nutres.2020.03.002.

Boschi, A., Uccelli, L. and Martini, P. (2019) 'A Picture of Modern Tc-99m Radiopharmaceuticals: Production, Chemistry, and Applications in Molecular Imaging', *Applied Sciences*, 9(12), p. 2526. doi: 10.3390/app9122526.

Budson, A. E. and Solomon, P. R. (2012) 'New Criteria for Alzheimer Disease and Mild Cognitive Impairment: Implications for the Practicing Clinician', *Neurologist*, 18(6), pp. 356–63. doi: 10.1097/NRL.0b013e31826a998d.

Chen, J. *et al.* (2016) 'Curcumin and its Promise as an Anticancer Drug: An Analysis of its Anticancer and Antifungal Effects in Cancer and Associated Complications from Invasive Fungal Infections', *European journal of pharmacology*, 772, pp. 33–42. doi: 10.1016/j.ejphar.2015.12.038.

Cui, M. *et al.* (2011) 'Synthesis and Structure−Affinity Relationships of Novel Dibenzylideneacetone Derivatives as Probes for β-Amyloid Plaques', *Journal of Medicinal Chemistry*, 5(7), pp. 2225–2240. doi: 10.1021/jm101404k.

Cunha, L. *et al.* (2014) 'The Role of Molecular Imaging in Modern Drug Development', *Drug Discovery Today*, 19(7), pp. 936–48. doi: 10.1016/j.drudis.2014.01.003.

Dubost, E. *et al.* (2020) 'Recent Advances in Synthetic Methods for Radioiodination', *The Journal of Organic Chemistry*, 85(13), pp. 8300–8310. doi: 10.1021/acs.joc.0c00644.

Effendi, N. *et al.* (2018) 'Radiobrominated Benzimidazole-Quinoline Derivatives as Platelet-Derived Growth Factor Receptor Beta (PDGFRβ) Imaging Probes', *Scientific Reports*, 8(1), p. 10369. doi: 10.1038/s41598-018-28529-0.

Effendi, N. *et al.* (2019) 'Design, Synthesis, and Biological Evaluation of Radioiodinated Benzo[*d*]imidazole-Quinoline Derivatives for Platelet-Derived Growth Factor Receptor β (PDGFRβ) Imaging', *Bioorganic & medicinal chemistry*, 27(2), pp. 383–393. doi: 10.1016/j.bmc.2018.12.016.

Fass, L. (2008) 'Imaging and Cancer: A Review', *Molecular Oncology*, 2(2), pp. 115–152. doi: 10.1016/j.molonc.2008.04.001.

Filippi, L. *et al.* (2018) '$^{18}$F-Labeled Radiopharmaceuticals for the Molecular Neuroimaging of Amyloid Plaques in Alzheimer's Disease', *American Journal of Nuclear Medicine and Molecular Imaging*, 8(4), pp. 268–281.

Galbán, C. *et al.* (2010) 'Applications of Molecular Imaging', *Progress in Molecular Biology and Translational Science*, 95, pp. 237–298. doi: 10.1016/B978-0-12-385071-3.00009-5 PMCID: PMC4327770 NIHMSID: NIHMS656933.

Heger, M. *et al.* (2014) 'The Molecular Basis for the Pharmacokinetics and Pharmacodynamics of Curcumin and its Metabolites in Relation to Cancer', *Pharmacological Reviews*, 66(1), pp. 222–307. doi: 10.1124/pr.110.004044.

Hewlings, S. J. and Kalman, D. S. (2017) 'Curcumin: A Review of Its' Effects on Human Health', *Foods*, 6(10), p. 92. doi: 10.3390/foods6100092.

International Atomic Energy Agency (IAEA) (2009) *Technetium-99m Radiopharmaceuticals: Status and Trends*. Vienna: Radioisotopes and Radiopharmaceuticals Series No. 1.

Jack, C. R. J. *et al.* (2018) 'NIA-AA Research Framework: Toward a Biological

Definition of Alzheimer's Disease', *Alzheimer's & dementia*, 14(4), pp. 535–562. doi: 10.1016/j.jalz.2018.02.018.

Kim, H. *et al.* (2019) 'Synthesis and in Vivo Characterization of $^{18}$F-Labeled Difluoroboron-Curcumin Derivative for β-Amyloid Plaque Imaging', *Scientific Reports*, 9, pp. 10.1038/s41598-019-43257–9. doi: 10.1038/s41598-019-43257-9.

Kumar, C., Subramanian, S. and Samuel, G. (2016) 'Evaluation of Radioiodinated Curcumin for its Potential as A Tumor-Targeting Radiopharmaceutical', *Journal of Radiation and Cancer Research*, 7(4), pp. 112–116. doi: 10.4103/0973-0168.199309.

Kunwar, A. *et al.* (2008) 'Quantitative Cellular Uptake, Localization and Cytotoxicity of Curcumin in Normal and Tumor Cells', *Biochimica et biophysica acta*, 1780(4), pp. 673–679. doi: 10.1016/j.bbagen.2007.11.016.

Lee, I. *et al.* (2011) 'Synthesis and Evaluation of 1-(4-[$^{18}$F]Fluoroethyl)-7-(4'-Methyl)Curcumin with Improved Brain Permeability for β-Amyloid Plaque Imaging', *Bioorganic & medicinal chemistry letters*, 21(19), pp. 5765–5769. doi: 10.1016/j.bmcl.2011.08.003.

Mankoff, D. A. (2007) 'A Definition of Molecular Imaging', *Journal of Nuclear Medicine*, 48(6), pp. 18N–21N.

Martiniova, L. *et al.* (2016) 'Gallium-68 in Medical Imaging', *Current radiopharmaceuticals*, 9(3), pp. 187–207. doi: 10.2174/1874471009666161028150654.

Orteca, G. *et al.* (2019) 'Development of A Potential Gallium-68-Labelled Radiotracer Based on DOTA-Curcumin for Colon-Rectal Carcinoma: from Synthesis to in Vivo Studies', *Molecules*, 24(3), p. 644. doi: 10.3390/molecules24030644.

Perrone, D. *et al.* (2015) 'Biological and Therapeutic Activities, and Anticancer Properties of Curcumin', *Experimental and Therapeutic Medicine*, 10(5), pp. 1615–1623. doi: 10.3892/etm.2015.2749.

Reiman, E. M. and Jagust, W. J. (2012) 'Brain Imaging in The Study of Alzheimer's Disease', *Neuroimage*, 61(2), pp. 505–516. doi: 10.1016/j.neuroimage.2011.11.075.

Rubagotti, S. *et al.* (2016) 'Affinity of $^{nat/68}$Ga-Labelled Curcumin and Curcuminoid Complexes for β-Amyloid Plaques: Towards the Development of New Metal-Curcumin Based Radiotracers', *International Journal of Molecular Sciences*, 17(9), p. 1480. doi: 10.3390/ijms17091480.

Ryu, E. K. *et al.* (2006) 'Curcumin and Dehydrozingerone Derivatives: Synthesis, Radiolabeling, and Evaluation for Beta-Amyloid Plaque Imaging', *Journal of Medicinal Chemistry*, 49(20), pp. 6111–6119. doi: 10.1021/jm0607193.

Sagnou, M. *et al.* (2011) 'Curcumin as the OO Bidentate Ligand in "2 + 1" Complexes with the $[M(CO)_3]^+$ (M = Re, $^{99m}$Tc) Tricarbonyl Core for Radiodiagnostic Applications', *Inorganic Chemistry*, 50(4), pp. 1295–1303. doi: 10.1021/ic102228u.

Shin, S. *et al.* (2015) 'Synthesis and Characterization of $^{18}$F-labeled Hydrazinocurcumin Derivatives for Tumor Imaging', *RSC Advances*, 5(117), pp. 96733–96745. doi: 10.1039/c5ra15380h.

Steven T DeKosky and Marek, K. (2003) 'Looking Backward to Move Forward: Early Detection of Neurodegenerative Disorders', *Science*, 302(5646), pp. 830–4. doi: 10.1126/science.1090349.

Takizawa, C. *et al.* (2015) 'Epidemiological and Economic Burden of Alzheimer's Disease: a Systematic Literature Review of Data Across Europe and the United States of America', *Journal of Alzheimer's disease*, 43(4), pp. 1271–84. doi: 10.3233/JAD-141134.

Triantis, C. *et al.* (2013) 'Synthesis and Characterization of *fac*-$[M(CO)_3(P)(OO)]$ and *cis-trans*-$[M(CO)_2(P)_2(OO)]$ Complexes (M = Re, $^{99m}$Tc) with Acetylacetone and Curcumin as OO Donor Bidentate Ligands', *Inorganic Chemistry*, 52(22), pp. 12995–3003. doi: 10.1021/ic401503b.

Uzuegbunam, B. C., Librizzi, D. and Yousefi, B. H. (2020) 'PET Radiopharmaceuticals for Alzheimer's Disease and Parkinson's Disease Diagnosis, the Current and Future Landscape', *Molecules*, 25(4), p. 977. doi: 10.3390/molecules25040977.

Walker, B. C. and Mittal, S. (2020) 'Antitumor Activity of Curcumin in Glioblastoma', *Internasional Journal of Molecular Sciences*, 21(24), p. 9435. doi: 10.3390/ijms21249435.

Zhao, J. *et al.* (2017) 'Curcumin Potentiates The Potent Antitumor Activity of ACNU Against Glioblastoma by Suppressing The PI3K/AKT and NF-κB/COX Signaling Pathways', *OncoTargets and Therapy*, 10, pp. 5471–5482. doi: 10.2147/OTT.S149708.

Zhu, H. *et al.* (2014) 'Curcumin Attenuates Acute Inflammatory Injury by Inhibiting The TLR4/MyD88/NF-κB Signaling Pathway in Experimental Traumatic Brain Injury', *Journal of Neuroinflammation*, 11(59). doi: 10.1186/1742-2094-11-59.